

ORIGINAL ARTICLE

Effect of trichosanthin on apoptosis and telomerase activity of nasopharyngeal carcinomas in nude mice

Min Kang¹, Hesheng Ou^{3*}, Rensheng Wang¹, Wenqi Liu¹, Yan Mao¹, Anzhou Tang^{2*}

¹Department of Radiology, ²Department of Otolaryngology, Head and Neck Surgery, First Affiliated Hospital of Guangxi Medical University, and ³Pharmacology College, Guangxi Medical University, Nanning, Guangxi, China

*Equal contributors to this study

Summary

Purpose: To evaluate the effect of trichosanthin (TCS) on telomerase activity and apoptosis in nasopharyngeal carcinoma cells implanted into nude mice.

Methods: Nude mice implanted with CNE1 and CNE2 nasopharyngeal carcinoma cell lines were randomly divided into 3 groups, including TCS group, control group (treatment with saline only), and cyclophosphamide (CTX) group. The weight of mice and the tumor volume were measured. The ultra-microstructural changes were observed by transmission electron microscope. Expression of Bcl-2 and Bax were investigated by immunohistochemistry. Apoptosis of CNE1 and CNE2 cells was determined by the TUNEL

method, and telomerase activity by TRAP-ELISA.

Results: Compared with the normal control group (saline group), TCS significantly inhibited the growth of both CNE1 and CNE2 tumor cells. CTX also inhibited the growth of both CNE1 and CNE2 tumor cells but this inhibition was slightly slower compared with the TCS.

Conclusion: TCS suppresses the growth of CNE1 and CNE2 cells lines in vivo. Its anticancer effects were associated with induction of apoptosis and, at least partially, with suppression of telomerase activity.

Key words: apoptosis, nasopharyngeal carcinoma, telomerase, trichosanthin

Introduction

Nasopharyngeal carcinoma occurs mainly in the coastal areas in China, such as Guangdong, Guangxi, Hunan, Jiangxi, and Fujian provinces. The incidence of nasopharyngeal carcinoma in Guangxi is around 10/100,000 population [1,2]. The main treatment for nasopharyngeal carcinoma is radiotherapy with 5-year overall survival rate of about 70%. Chemotherapy is also an important option for such patients, especially for those in the late stages. However, because of the toxicity of chemotherapy, it is hard to get the desired therapeutic effect. Therefore, more effective drugs with fewer side effects for nasopharyngeal carcinoma are needed.

TCS, a type I ribosome-inactivating protein, is isolated from the root tubers of the Chinese me-

dicinal herb *Trichosanthes kirilowii* Maximowicz, which has been used as an abortifacient for 1,500 years in China because of its high toxicity on trophoblasts [3]. In the past 20 years, TCS grasped the interest of many researchers by virtue of its potential antitumor activities showing cytotoxicity in a variety of tumor cells, such as breast cancer, cervical cancer and chronic myelogenous leukemia [4-6]. TCS has been considered as a potential biological agent for cancer treatment. The possible mechanisms of its biological function could be attributed to inhibition of protein synthesis and consequently induction of necrosis, as well as induction of apoptosis in several tumor cell lines [7-12]. Although TCS-induced apoptosis of tumor cell lines is now well known, the underlying mechanisms remain to be elucidated. Recent data showed that telomerase activity might

be involved in the regulation of cancer cell proliferation and apoptosis [13-15].

Telomeres maintain genomic stability by protecting the linear chromosome ends from being recognized as DNA breaks that would need repair. They undergo frequent remodeling during important biological procedures including development, proliferation, and neoplastic transformation [16]. The telomeric TTAGGG repeats are replenished by telomerase, which is a ribonucleoprotein complex consisting of a catalytic reverse transcriptase protein subunit (e.g. TERT) [17], a template RNA (e.g. TERC) [18], dyskerin [19], and other accessory proteins [20]. Telomerase is the enzyme responsible for the maintenance of the length of telomeres by adding guanine-rich repetitive sequences. Telomerase activity is exhibited in gametes and stem and tumor cells. In human somatic cells, proliferation potential is strictly limited and senescence follows approximately 50-70 cell divisions. On the contrary, in most tumor cells replication potential is unlimited [21]. Proliferating cells such as embryonic stem and cancer cells display high telomerase activity regulated primarily at the level of hTERT transcription [22].

In the present study, using the nasopharyngeal carcinoma cell lines CNE1 and CNE2 implanted in nude mice, we investigated the effect of TCS on the nasopharyngeal carcinoma cell growth, and the molecular mechanisms underlying the telomerase activity and apoptosis.

Methods

Cells and reagents

Nasopharyngeal carcinoma cell lines CNE1 and CNE2 were cultured in IMDM medium with 10% newborn calf serum, 100 U·mL⁻¹ penicillin and 100 U·mL⁻¹ streptomycin in incubator at 37 °C with 5% CO₂. Used were 60 BALB/C-nu/nu nude mice (half males, half females), weighing 18-22 g and aged 4-5 weeks. The mice were germ-free and of non-lymphocytic immunodeficiency type. The animals were purchased from the Institute of Animals, Chinese Academy of Sciences in Beijing, and fed under specific pathogen free (SPF) condition. TCS was purchased from Tonghua Baishan Pharmaceutical Company (Tonghua, China). The concentrations of TCS used in this study were 10, 20, 30, 40, and 50 mg/l. Cyclophosphamide was purchased from the German Baxter Pharmaceutical Company. Iscove's media (IMDM), newborn calf serum and trypsin were purchased from Gibco (Grand Island, NY, USA). TUNEL kits were purchased from Roche Pharmaceutical (Branchburg, NJ, USA). TRAP-ELISA kits were purchased from Chemicon International Inc (Temecula, CA, USA). Bcl-2

(MAB20014), Bax (MAB20254), Ultrasensitive TM, S-P Plus Kit, and DAB were purchased from Fuzhou Maixin Company (Fuzhou, China). Electron microscope was Japanese JEM-1200EX transmission electron microscope. The flow cytometry FACSCaLibur was purchased from American Beckman Coulter Company (California, CA, USA).

Animal model

The CNE1 or CNE2 cells in logarithmic phase were digested by trypsin and made a cell suspension of 5×10^7 /ml. Each mouse was inoculated with 0.2 ml of cell suspension in the armpit, and in situ tumor growth appeared about 1 week after inoculation. When tumors grew to 0.687 ± 0.420 cm³, the animals were randomly divided into 3 groups: TCS group, CTX group and control group. Intragastric doses were calculated according to the formula [23] $dB = dA \times (RB/RA) \times (WA/WB) 1/3$, where dB was the mouse dosage, dA the human dose, R was the animal shape coefficient (RA was 1.00 and RB 0.59). WA was the average human weight and WB was the mouse weight. The dosage of TCS was 15 mg/kg once a day. The control group was gavaged for identical volume of saline. The CTX group received 0.2 µg/kg of CTX with intraperitoneal injection 3 times a day. During treatment, the weight and size of tumors were measured every 3 days. The longest (a) and shortest (b) tumor diameters were measured by vernier caliper and volume (V) was calculated as $V/\text{cm}^3 = \pi ab^2/6$ [24]. Thirty days after treatment mice were euthanized. Tumor tissue was taken and weighed and the tumor inhibition rate was calculated as follows: Tumor inhibition rate (%) = $[1 - (\text{average tumor weight of treatment group} / \text{average tumor weight of control group})] \times 100\%$ [25]. Relative tumor volume: $RTV = V_t / V_0$. V_t was the tumor volume at the end of the experiment. V_0 was the initial tumor volume. The relative tumor growth rate (%) was calculated as follows: $T / C = RTV_{\text{experimental group}} / RTV_{\text{control group}} \times 100\%$.

Immunohistochemical detection

The tumor tissue was immunohistochemically stained with streptavidin/peroxidase (SP), with PBS as rinsing liquid. After being colored with 3,3'-diaminobenzidine (DAB), tumor tissue was redyed with hematoxylin. Positive reaction (+) was defined as brown granules in the cytoplasm. The expression intensity was expressed as positive cell proportion and color intensity [26].

TUNEL detection

Mediated by terminal deoxynucleotidyl transferase, the dUTP-labeling method was applied as kit reference. Brown or red granules in the nucleus defined positive (apoptotic) tumor cells and blue showed surviving tumor cells. At least three high power fields and more than 500 intact cancer cells were observed

at each section. The number of positive cells per 100 cancer cells defined the apoptosis index (AI).

Flow cytometry

The cell debris of tumor tissue were removed by 200 r/s centrifugation and fully washed by PBS. Filtered by 300-mesh strainer, single-cell suspension was prepared. The cell cycle data were processed by BD MultiCycle software (Beckman Coulter, Fullerton, CA, USA) [27].

Transmission electron microscopy

Tumor tissue was taken and fixed by 4% glutaraldehyde and 1% osmium tetroxide. Dehydrated by alcohol and acetone, it was embedded in epoxy resin and cut into 0.5 μm thickness slices. After staining with uranyl acetate and lead citrate, tissue was observed by JEM-1200EX transmission electron microscope.

TRAP-PCR-ELISA

Tumor tissue of 100 mg was taken and grinded by liquid nitrogen. After fully cracked by 200 μl of pre-cooling lysate, tumor tissue was centrifuged to 12000 rpm for 20 min. The supernatant was taken and stored at $-80\text{ }^{\circ}\text{C}$. The protein concentration was adjusted to 10 $-500\text{ ng}\cdot\mu\text{L}^{-1}$. Two μl of extracted tumor tissue protein and 2 μl of heat-processed extracted liquid were added to the 50 μl reaction system, including 10 μl of 5 \times TRAP reaction liquid, 0.4 μl of Taq enzyme (5 \times 106 U/l), and 37.6 μl of DEPC water. The product was amplified at 94 $^{\circ}\text{C}$ for 30 sec and at 55 $^{\circ}\text{C}$ for 30 sec for 33 cycles. Five μl of PCR product was added to hybridization solution of 100 μl , and coated in the anti digoxin ELISA plate at 37 $^{\circ}\text{C}$ for 1 h with peroxidase. Avoiding light, after incubation for 30 min at room temperature, the product

was colored with TMB chromogenic substrate for 10 min and termination solution was added to terminate the reaction. Absorption values at the wavelength of 450 nm and 690 nm were measured by enzyme-labeled instrument. $A = A_{450} - A_{690}$, $A = A_{\text{sample}} - A_{\text{heat treatment sample}}$. $A > 0.15$ was considered as telomerase positive.

Statistics

Data was processed by SPSS 13.0 statistical software (SPSS Inc. Chicago, IL, USA). The tumor growth curve was repeatedly measured for variance analysis. Body weight, tumor inhibition rate, apoptosis rate, cell cycle change and telomerase activity in tumor tissue between different groups were analyzed with single factor analysis. The positive rate of telomerase activity was analyzed by the χ^2 test.

Results

The effects of TCS on tumor growth

To investigate the effect of TCS on tumor growth, the tumor size was determined in a time course manner. Thirty days after administration, tumor growth in each tumor-bearing nude mice group in the CTX and TCS groups was slower than that in the normal saline control group. The tumor growth in the CTX group was slightly slower compared with the TCS group, as shown in Figure 1.

The effects of TCS on weight and transplanted tumor weight in nude mice

To further analyze the effect of TCS on tumor growth, the transplanted tumor weight was deter-

Table 1. The effect of TCS on weight and transplanted tumor weight of CNE1 and CNE2 nude mice (mean \pm standard deviation, N = 10)

Groups	Weight (g)		Tumor volume (cm^3)		Tumor weight (g)	Tumor inhibition rate (%)	RTV	T/C (%)
	Before treatment	After treatment	Before treatment	After treatment				
CNE1 TCS group	21.0 \pm 0.7	26.8 \pm 3.6*	0.558 \pm 0.174	3.832 \pm 0.82*	6.82 \pm 1.02*	38.7	6.9 \pm 1.4*	38.1
CNE1 CTX group	20.7 \pm 1.1	27.9 \pm 1.7**	0.702 \pm 0.334	2.073 \pm 0.531**	3.43 \pm 0.92**	69.2	3.6 \pm 1.6**	19.9
CNE1 control group	20.7 \pm 1.4	30.5 \pm 1.9	0.687 \pm 0.420	9.613 \pm 1.387	11.13 \pm 1.02		18.1 \pm 8.3	
CNE2 TCS group	21.0 \pm 0.8	24.5 \pm 2.6*	0.458 \pm 0.153	8.802 \pm 0.801*	7.61 \pm 1.32*	46.7	19.2 \pm 3.4*	57.7
CNE2 CTX group	21.8 \pm 1.1	25.6 \pm 1.7*	0.957 \pm 0.490	5.198 \pm 0.384**	5.47 \pm 0.40**	61.7	6.6 \pm 3.0**	38.4
CNE2 control group	21.6 \pm 1.1	29.0 \pm 1.4	0.861 \pm 0.280	13.713 \pm 2.641	14.27 \pm 0.52		17.2 \pm 5.9	

* $p < 0.05$, ** $p < 0.01$. Tumor inhibition rate $> 30\%$ and T/C $< 60\%$ were considered significant in antitumor drug screening [4]. RTV: relative tumor volume, T/C: RTV exper/RTV control, CTX: cyclophosphamide

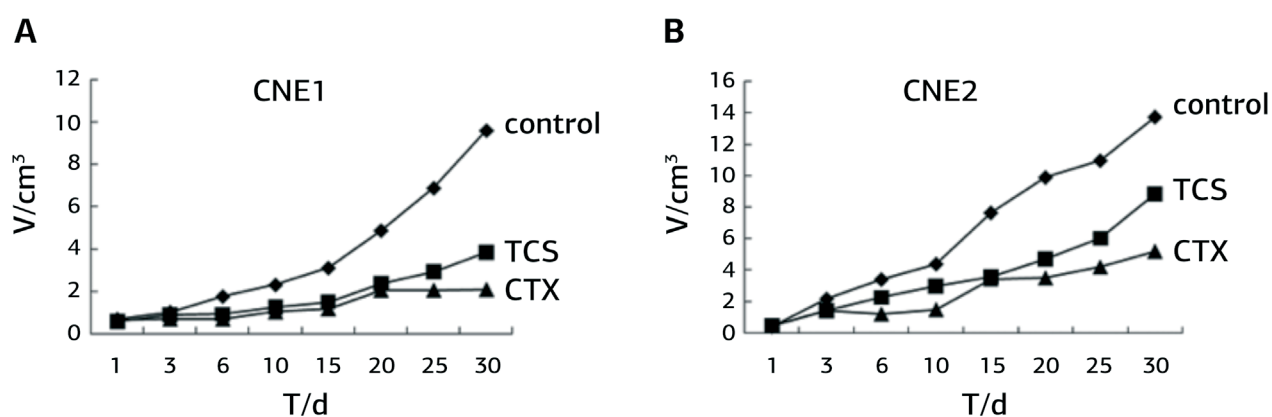


Figure 1. The effect of TCS on tumor growth curve of tumor-bearing nude mice. The tumor size of each tumor-bearing nude mouse was determined in 30 days. The longest (A) and shortest (B) diameters of the tumor were measured by vernier caliper. The volume (V) was calculated as $V/\text{cm}^3 = \pi ab^2/6$; T/d: days of treatment time; cm^3 : tumor volume. TCS vs saline control group, $p < 0.01$; CTX vs saline control group, $p < 0.01$; TCS vs CTX, $p > 0.05$.

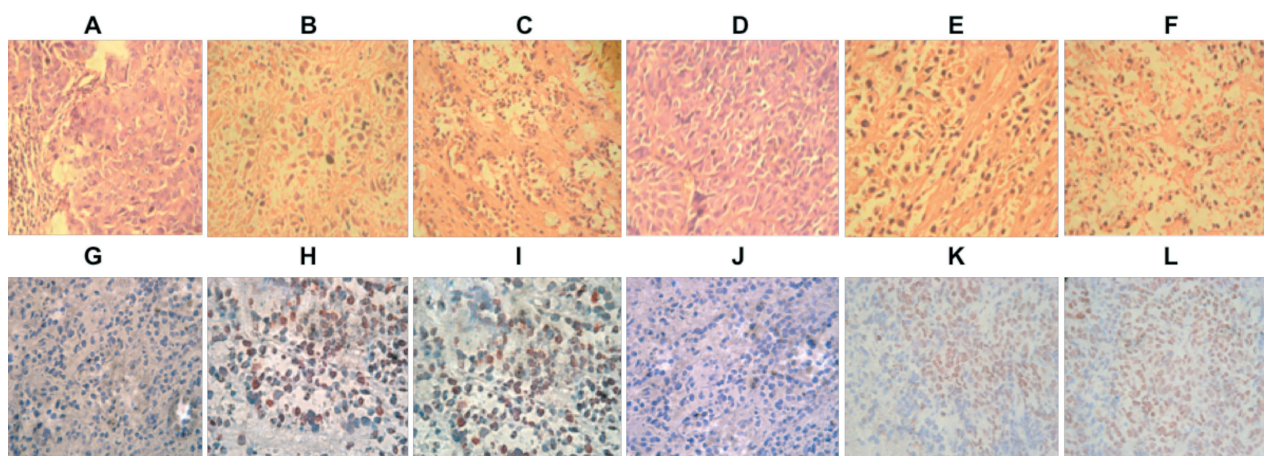


Figure 2. The effect of TCS on tumor tissue of nude mice. (A-F): The effect of TCS on morphological change in tumor tissue of nude mice (H&E staining $\times 400$). (A): CNE1 control group; (B): CNE1 TCS group; (C): CNE1 CTX group; (D): CNE2 control group: tumor cell grew expansively and proliferated actively; (E): CNE2 TCS group; (F): CNE2 CTX group, (G-L): The apoptotic effect of TCS on implanted tumor (Tunel staining $\times 400$); (G): CNE1 control group; (H): CNE1 TCS; (I): CNE1 CTX group; (J): CNE2 control group; (K): CNE2 TCS group; (L): CNE2 CTX group.

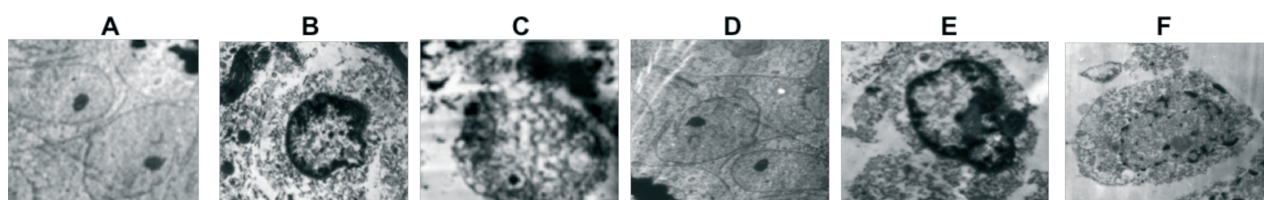


Figure 3. The effect of TCS on the ultrastructure of CNE1 and CNE2 implanted tumor in nude mice. (A): CNE1 control group: there are lots of cancer cells with clear nucleus. No apoptotic cells are seen ($\times 2200$). (B): CNE1 TCS group: there are apoptotic cells with condensed nuclear chromatin, edge phenomenon and less organelles ($\times 8800$). (C): CNE1 CTX group: there are pyknosis, dissolving of homogenization and nuclear fragmentation in the late stage ($\times 2800$). (D): CNE2 control group: there are abnormal nucleus, visible nucleoli, abundant villi and small vacuoles in the cytoplasm ($\times 2200$). (E): CNE2 TCS group: there are apoptotic cells with condensed nuclear chromatin, edge phenomenon and less organelles ($\times 3800$). (F): CNE2 CTX group: there are fragmented nucleus and ruptured cell membrane ($\times 3800$).

Table 2. The apoptosis effect of TCS on CNE1 and CNE2 implanted tumor (mean± standard deviation, N=20)

Groups	CNE1	CNE2
TCS group	48.2 ± 1.6*	61.1 ± 1.3*
CTX group	61.7 ± 1.2*	89.4 ± 0.4*
Control group	1.9 ± 0.9	2.8 ± 1.1

*p < 0.01 when compared with the control group

Table 3. The effect of TCS on Bcl-2 and Bax of xenografts in nude mice (mean± standard deviation, N=10)

Groups	Bcl-2 (%)	Bax (%)
CNE1 TCS group	29.9 ± 3.0*	56.5 ± 0.5*
CNE1 CTX group	22.1 ± 4.3**	63.0 ± 8.5**
CNE1 control group	61.4 ± 6.0	16.2 ± 6.3
CNE2 TCS group	30.6 ± 2.4*	53.9 ± 3.2*
CNE2 CTX group	11.2 ± 4.6**	68.0 ± 9.1**
CNE2 control group	56.2 ± 5.0	25.7 ± 6.1

*p < 0.05, **p < 0.01

mined. As shown in Table 1, there was no death in all groups, and weight loss in the TCS group was 20% less compared to the normal saline control group. There was significant tumor inhibition with TCS in mice implanted with CNE1 or CNE2 cells, with tumor inhibition rates of 38.7 and 46.7%, respectively (compared with the normal saline control group, $p < 0.01$). Tumor inhibition rates in the CTX group were 69.2 and 61.7%, respectively (compared with the normal saline control group, $p < 0.01$). The inhibitory effects of TCS on tumor growth were slightly less compared to CTX ($p > 0.05$, Table 1).

The effects of drugs on the morphological change in the two kinds of tumor tissue cells

To investigate the pharmacological effect of TCS on tumor cells, tissues were stained with hematoxylin/eosin (HE) (Figure 2, A-F). HE staining showed that cells in the two tumor tissue control groups shared enlarged nuclear/cytoplasmic ratio, cell nuclear hyperchromatism, increased split phase, stronger heterogeneity, and tumor grew expansively with partial necrosis of the central cells. Cells in TCS group showed different degrees of nuclear pyknosis with morphology of circular, polygonic, bar, ring and crescents. Cells in split phase were fewer with massive lymphocytic infiltration. The tumor cell proportion was reduced and wrapped by a large number of fibroblasts. TCS killed tumor cells and inhibited tumor cell division to a certain degree (Figure 2, A-F).

The effects of TCS on tumor cell apoptosis

The effect of TCS on tumor cell apoptosis

was measured by TUNEL assay and the results are shown Table 2. Single factor variance analysis showed obvious apoptotic effect of TCS, when compared with the normal saline control group ($p < 0.01$) as shown in Figure 2, G-L.

The ultrastructure of tumor cells determined by transmission electron microscopy

To observe the alterations of ultrastructure of tumor cell, transmission electron microscope was used in this study (Figure 3). Cells in the control groups were irregular in shape with abundant villi, clear organelle structure, irregular nuclear shape, enlarged nuclear/cytoplasmic ratio, and rich intranuclear heterochromatin. In the TCS group, cells showed typical apoptosis, small cell variance, still intact structure, high density of cytoplasm, nuclear shrinking, condensed nuclear chromatin and edge phenomenon. In the CTX group, cells showed pyknosis, dissolving of homogenization and nuclear fragmentation. There were vacuoles in the cytoplasm, rupture of the cell membrane and cellular debris.

The effects of TCS on the expression of Bax and Bcl-2 in tumor tissues

To further analyze the potential molecular mechanism(s) involved in the effect of TCS on cell apoptosis, the tissue levels of Bax and Bcl-2 were determined. The expression of Bcl-2 protein in the TCS group was lower than that of the control group ($p < 0.01$), while Bax expression was significantly higher than that of the control group ($p < 0.01$) with deep brown color in the cytoplasm. These showed the decreased ratio of Bax and Bcl-2 after administration of TCS (Table 3).

The effects of TCS on tumor cell cycle

As shown in Table 4, in the CNE1 cell line treatment with TCS resulted in increase in G0+G1 by 23.5 % (60.4 ± 1.1 vs 48.9 ± 0.6 ; $p < 0.01$), and the AI showed a 14.4-fold increase (41.6 ± 6.5 vs 2.7 ± 2.6 ; $p < 0.01$) compared with the normal saline control group. The same results were observed in the CNE2 cell line, in which G0+G1 increased by 42.1 % (60.8 ± 0.4 vs 42.8 ± 1.1 ; $p < 0.01$), and the AI showed 19.5-fold increase (59.5 ± 3.9 vs 2.9 ± 2.6 ; $p < 0.01$) compared with the normal saline control group.

The detection and analysis of telomerase activity in nude mice

To explore whether the telomerase activity was involved in the cell growth, the levels of

Table 4. The effect of TCS on tumor cell cycle and apoptosis rate of CNE1 and CNE2 implanted tumor in nude mice (mean± standard deviation, N=10)

Groups	Cell cycle (%)			AI (%)
	G ₀ + G ₁	S	G ₂ + M	
CNE1 TCS group	60.4 ± 1.1*	34.6 ± 0.9	5.0 ± 0.4*	41.6 ± 6.5*
CNE1 CTX group	70.0 ± 0.6*	23.2 ± 0.6*	6.8 ± 0.4*	77.9 ± 9.7*
CNE1 control group	48.9 ± 0.6	35.6 ± 0.9	15.5 ± 0.7	2.7 ± 2.6
CNE2 TCS group	60.8 ± 0.4*	15.0 ± 0.6*	24.2 ± 1.1*	59.5 ± 3.9*
CNE2 CTX group	68.2 ± 0.9*	12.9 ± 0.6*	18.9 ± 0.4*	69.6 ± 6.3*
CNE2 control group	42.8 ± 1.1	25.6 ± 0.5	31.6 ± 0.6	2.9 ± 2.6

*p < 0.01, AI: apoptotic index

the enzyme in tumor tissue were determined by ELISA. As can be seen in Table 5, after treatment with TCS telomerase activity was significantly decreased (4.1-fold; 0.035 ± 0.019 vs 0.179 ± 0.01 ; $p < 0.05$) in the CNE1, and by 1.27-fold (0.093 ± 0.014 vs 0.211 ± 0.037 ; $p < 0.05$) in the CNE2, compared with the normal saline control group. These results indicated that the telomerase activity was inhibited in both CNE1 and CNE2 cell lines.

Discussion

Under normal circumstances, cell proliferation and apoptosis are maintained in equilibrium, and cancer results from imbalance of cell proliferation and apoptosis. Mutations in malignant cells make them to circumvent the limitations and lead to unlimited proliferation. The length of telomere determines the limits of proliferation of normal cells, while the high telomerase activity of tumor cells results in their continuous proliferation. This reveals that apoptosis and telomerase expression are influential in tumor genesis and development. Therefore induction of tumor cells' apoptosis and inhibition of telomerase activity are considered a new approach to cancer treatment. It was reported [28] that activation of telomerase is essential for the uncontrolled proliferation of malignant cells which activate telomerase activity to maintain telomere length to prevent cell death. Since most tumor cells express telomerase activity, which is not expressed by normal cells [29], inhibiting telomerase activity may be a breakthrough for cancer treatment. Many synthetic compounds and natural products have shown a preventive activity, and some even have entered clinical trials, such as polyphenols and flavonoids [30]. Recently, anticancer drugs from plant sources have become more and more popular. The antitumor effect of some of them has been shown [31], and

herbs extracts become increasingly popular for cancer treatment [32-35]. South America antitumor drugs R&D Department set relevant standards for the plant extracts, and $IC_{50} \leq 50 \text{ mg} \cdot \text{L}^{-1}$ of plant extracts *in vitro* is characterized as effective antitumor activity [36]. In the present study, the effects of TCS on nasopharyngeal carcinoma were explored in terms of morphology and function. It was found that tumor growth was significantly inhibited ($p < 0.01$). The animals' skin was drier and dark red in the positive control group (CTX group) than in the TCS group, which indicates less side effects and better animals' quality of life with TCS compared with conventional Western medicine. TCS-induced tumor cell apoptosis and flow cytometry revealed increased cell apoptosis rate and decreased propidium iodide (PI) index, indicating inhibition of cell DNA synthesis. Cells were blocked in the G₀/G₁ phase, and cells in S and G₂/M phase were reduced, implying that tumor growth was suppressed.

The Bcl-2 family is the most important gene family for apoptosis regulation. The ratio of Bcl-

Table 5. The effect of TCS on telomerase activity in nude mice

Groups	N	Mean±standard deviation	Positive rate (%)
CNE1 TCS group	10	$0.035 \pm 0.019^*$	0 (0/10)*
CNE1 CTX group	10	$0.046 \pm 0.011^{**}$	0 (0/10)**
CNE1 control group	10	0.179 ± 0.010	100 (10/10)
CNE2 TCS group	10	$0.093 \pm 0.014^*$	0 (0/10)*
CNE2 CTX group	10	$0.099 \pm 0.056^{**}$	20 (2/10)**
CNE2 control group	10	0.211 ± 0.037	100 (10/10)

Each group was compared with the control group. *p < 0.05, ** p < 0.01

2 and Bax is considered to be the key point for cell apoptosis. Heteroduplex of Bcl-2 and Bax prevents apoptosis [37]. When Bax is intracellularly overexpressed, the Bax/Bax ratio is greater than the Bcl-2/Bax ratio, which promotes cell apoptosis [38]. In addition, high expression of Bcl-2 may also reduce ultraviolet (UV), etoposide (VP16) and cyclophosphamide (CP) induced cell death, but cell cycle would not be blocked [38]. In the present study it was shown that after administration of TCS, the Bcl-2 protein expression was significantly lower than that of the normal saline control group ($p < 0.01$), and Bax expression was significantly higher than that of the control group ($p < 0.01$) with deepened cytoplasmic brownish coloring. This indicates that the Bax and Bcl-2 ratio was reduced because of TCS, and therefore cell apoptosis was promoted.

The effect of telomerase on tumor genesis and progression is a research hotspot. Herbert et al. [39] found that activation of telomerase is an early event for tumor genesis, and chemopreventive agents, such as tamoxifen, inhibit telomerase

activity, so that telomerase activity is an effective marker for chemoprevention. Mori et al. [40] found, besides cell proliferation markers, that some new markers such as apoptosis and telomerase activity are also very important and can be used for tumor screening if combined with animal models.

This study explored the effect of TCS on telomerase activity in CNE1 and CNE2 nasopharyngeal carcinoma cell lines implanted in nude mice and showed significantly lower telomerase activity in the TCS group than that of the normal saline control group ($p < 0.01$). Because of the low toxicity and low price of TCS, it may be a potential natural medicine agent to induce tumor cell apoptosis and inhibit telomerase activity.

Acknowledgement

This study was supported by grants from the Department of Guangxi Science and Technology, China (No. 0322024-1A) and the National Natural Science Foundation of China (No. 30871186).

References

1. Jeannel D, Bouvier G, Huber A. Nasopharyngeal carcinoma: an epidemiological approach to carcinogenesis. *Cancer Surv* 1999; 33: 125-155.
2. Parkin DM, Bray F, Ferlay J, Pisani P. Global cancer statistics, 2002. *CA Cancer J Clin* 2005; 55: 74-108.
3. Jin YC. Clinical study of trichosanthin. In: Chang HM, Yeung HW, Tso WW, Koo A (Eds): *Advances in Chinese medicinal material research*. Singapore: World Scientific Publications Co, 1985; pp 319-326.
4. Ding NB, Chen DJ, Li XR, Hu G. Trichosanthin inhibits growth of breast cancer cells in vitro and in vivo. *J Pract Oncol* 2008; 23: 310-313.
5. Wang P, Li JC. Trichosanthin-induced specific changes of cytoskeleton configuration were associated with the decreased expression level of actin and tubulin genes in apoptotic HeLa cells. *Life Sci* 2007; 81: 1130-1140.
6. Zhang K, Xu J, Huang X et al. Trichosanthin down-regulated p210Bcr-Abl and enhanced imatinib-induced growth arrest in chronic myelogenous leukemia cell line K562. *Cancer Chemother Pharmacol* 2007; 60: 581-587.
7. Fang EF, Zhang CZ, Zhang L et al. Trichosanthin inhibits breast cancer cell proliferation in both cell lines and nude mice by promotion of apoptosis. *PLoS One* 2012; 7: e41592.
8. Huang Y, Song H, Hu H, Cui L, You C, Huang L. Trichosanthin inhibits DNA methyltransferase and restores methylation-silenced gene expression in human cervical cancer cells. *Mol Med Report* 2012; 6: 872-878.
9. Cai Y, Xiong S, Zheng Y, Luo F, Jiang P, Chu Y. Trichosanthin enhances anti-tumor immune response in a murine Lewis lung cancer model by boosting the interaction between TSLC1 and CRTAM. *Cell Mol Immunol* 2011; 8: 359-367.
10. Wang P, Xu S, Zhao K, Xiao B, Guo J. Increase in cytosolic calcium maintains plasma membrane integrity through the formation of microtubule ring structure in apoptotic cervical cancer cells induced by trichosanthin. *Cell Biol Int* 2009; 33: 1149-1154.
11. He JF, Li JC. The growth inhibition and the apoptosis of HeLa cells induced with TCS. *Acta Anatomica Sinica* 2006; 37: 301-314.
12. Higuchi S, Tamura T, Oda T. Cross-talk between the pathways leading to the induction of apoptosis and the secretion of tumor necrosis factor-alpha in ricin-treated RAW 264.7 cells. *J Biochem* 2004; 134: 927-933.
13. Symonds EL, Konczak I, Fenech M. The Australian fruit Illawarra plum (*Podocarpus elatus* Endl., Podocarpaceae) inhibits telomerase, increases histone

- deacetylase activity and decreases proliferation of colon cancer cells. *Br J Nutr* 2012; 15: 1-9.
14. Lai XF, Shen CX, Wen Z et al. PinX1 regulation of telomerase activity and apoptosis in nasopharyngeal carcinoma cells. *J Exp Clin Cancer Res* 2012; 31: 12.
 15. Sharma V, Koul N, Joseph C, Dixit D, Ghosh S, Sen E. HDAC inhibitor, scriptaid, induces glioma cell apoptosis through JNK activation and inhibits telomerase activity. *J Cell Mol Med* 2010; 14: 2151-2161.
 16. Blackburn EH. Switching and signaling at the telomere. *Cell* 2001; 106: 661-673.
 17. Harrington L, McPhail T, Mar V et al. A mammalian telomerase-associated protein. *Science* 1997; 275: 973-977.
 18. Blasco MA, Funk W, Villeponteau B, Greider CW. Functional characterization and developmental regulation of mouse telomerase RNA. *Science* 1995; 269: 1267-1270.
 19. Cohen SB, Graham ME, Lovrecz GO, Bache N, Robinson PJ, Reddel RR. Protein composition of catalytically active human telomerase from immortal cells. *Science* 2007; 315: 1850-1853.
 20. Venteicher AS, Abreu EB, Meng Z et al. A human telomerase holoenzyme protein required for Cajal body localization and telomere synthesis. *Science* 2009; 323: 644-648.
 21. Gauthier LR, Granotier C, Soria JC et al. Detection of circulating carcinoma cells by telomerase activity. *Br J Cancer* 2001; 84: 631-635.
 22. Wang S, Zhu J. Evidence for a relief of repression mechanism for activation of the human telomerase reverse transcriptase promoter. *J Biol Chem* 2003; 278: 18842-18850.
 23. Shuyun Xu (Ed). *The pharmacological experimental methodology*. Beijing, People's Health Press, 1996, pp 87-89.
 24. Wedge SR, Ogilvie DJ, Dukes M et al. ZD4190: An orally active inhibitor of vascular endothelial growth factor signaling with broad-spectrum antitumor efficacy. *Cancer Res* 2000; 60: 970-975.
 25. Okuno S, Harada M, Yano T et al. Complete regression of xenografted human carcinomas by camptothecin analogue-carboxymethyl dextran conjugate (T-0128). *Cancer Res* 2000; 60: 2988-2995.
 26. Zhou HB, Cai TJ, Li ML. White veratryl alcohol-induced apoptosis of human primary gastric cancer cell xenografts in nude mice. *Pathophysiology* 2005; 21: 528-532.
 27. Ding J, Miao ZH. *Drug Evaluation: guiding principles and methods*. In: Yongsu Zhen (Ed): *Anticancer drug research and development*. Beijing, Chemical Industry Press, 2004, pp 724-727.
 28. Rhyu MS. Telomeres, telomerase and immortality. *J Natl Cancer Inst* 1995; 87: 884-887.
 29. Kim NW. Clinical implication of telomerase in cancer. *Eur J Cancer* 1997; 33: 5781-5786.
 30. Khaw AK, Yong JW, Kalthur G, Hande MP. Genistein induces growth arrest and suppresses telomerase activity in brain tumor cells. *Genes Chromosomes Cancer* 2012; 51: 961-974.
 31. Spaulding-Albright N. A review of some herbs and relative products commonly used in cancer patients. *J Am Diet Assoc* 1997; 97: 208-213.
 32. Lee KH. Novel antitumor agents from higher plants. *Med Res Rev* 1999; 19: 569-596.
 33. Devi PU. *Withania Sornnifera Dunal (A shwagandha): Potential plant source of a promising drug for cancer chemotherapy and radiosensitization*. *Indian J Exp Biol* 1996; 34: 927-932.
 34. Han MQ, Liu JX, Gao H. Effects of 24 chinese medicinal herbs on nucleic acid, protein and cell cycle of human lung adenocarcinoma cell. *Zhong guo Zhong xi yi Jiehe Zazhi (Chin J Integr Tradit West Med)* 1995; 15: 147-149.
 35. Zhang F, Cui YH, Cao P. Proliferation inhibition and induction of apoptosis of quercetin on human nasopharyngeal carcinoma HEN1 cells. *Clin Otolaryngol Head Neck Surg* 2007; 21: 1136-1139.
 36. Mans DR, da Rocha AB, Schwartzmann G. Anti-cancer drugs discovery and development in Brazil: Targeted plant collection as a rational strategy to acquire candidate anticancer compounds. *Oncologist* 2000; 5: 185-198.
 37. Haraguchi M, Torii S, Matzuzawa SI et al. Apoptotic protease activating factor 1 (APAF 1)-independent cell death suppression by Bcl-2. *J Exp Med* 2000; 191: 1709-1720.
 38. Kim SC, Park SY, Kang HK et al. The Cytotoxicity of *Scytosiphon lomentaria* Against HL-60 Promyelocytic Leukemia Cells. *Cancer Biother Radiopharmac* 2004; 19: 641-648.
 39. Herbert BS, Wright AC, Passons CM et al. Effects of chemo-preventive and antitelomerase agents on the spontaneous immortalization of breast epithelial cells. *J Natl Cancer Inst* 2001; 93: 39-45.
 40. Mori H, Sugie S, Yoshimi N et al. Control of cell proliferation in cancer prevention. *Mut Res* 1999; 16: 291-298.